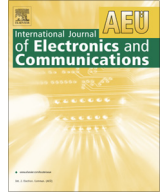




Contents lists available at ScienceDirect

International Journal of Electronics and Communications (AEÜ)

journal homepage: www.elsevier.com/locate/aeue

Regular paper

User clustering and robust beamforming design in multicell MIMO-NOMA system for 5G communications



Sunil Chinnadurai^a, Poongundran Selvaprabhu^a, Yongchae Jeong^a, Abdul Latif Sarker^a, Han Hai^a, Wei Duan^b, Moon Ho Lee^{a,*}

^a Institute of Information and Communication, Chonbuk National University, 664-14 Deokjin-dong, Jeonju 561-756, Republic of Korea

^b Department of Electronics and Communication Engineering, Nantong University, PR China

ARTICLE INFO

Article history:

Received 20 January 2017

Accepted 12 May 2017

Keywords:

MIMO

NOMA 5G

Robust beamforming design

User clustering

Power allocation

Weighted sum-rate

Optimization

ABSTRACT

In this paper, we present a robust beamforming design to tackle the weighted sum-rate maximization (WSRM) problem in a multicell multiple-input multiple-output (MIMO) – non-orthogonal multiple access (NOMA) downlink system for 5G wireless communications. This work consider the imperfect channel state information (CSI) at the base station (BS) by adding uncertainties to channel estimation matrices as the worst-case model i.e., singular value uncertainty model (SVUM). With this observation, the WSRM problem is formulated subject to the transmit power constraints at the BS. The objective problem is known as non-deterministic polynomial (NP) problem which is difficult to solve. We propose an robust beamforming design which establishes on majorization minimization (MM) technique to find the optimal transmit beamforming matrix, as well as efficiently solve the objective problem. In addition, we also propose a joint user clustering and power allocation (JUCPA) algorithm in which the best user pair is selected as a cluster to attain a higher sum-rate. Extensive numerical results are provided to show that the proposed robust beamforming design together with the proposed JUCPA algorithm significantly increases the performance in term of sum-rate as compared with the existing NOMA schemes and the conventional orthogonal multiple access (OMA) scheme.

© 2017 Elsevier GmbH. All rights reserved.

1. Introduction

The swift expansion of smart devices will lead to enormous amount of increase in data traffic for 5G communication systems [1,2]. Moreover, the requirement of higher data rates, lower latency, massive connectivity and high spectral efficiency poses a great challenge for 5G communication systems. To fulfill the aforementioned requirements, various key technologies such as millimeter (mm) wave [3,4], non-orthogonal multiple access (NOMA) [5] and massive multiple-input multiple-output (MIMO) [6,7] have been largely considered. Especially, NOMA has attained significant attraction in recent years to support fiercely increased network capacity with confined spectrum [8–10]. NOMA utilizes the same radio resources to serve multiple users simultaneously which yields better throughput, fairness, spectral efficiency than the conventional orthogonal multiple access (OMA) schemes

[11–14]. In particular, NOMA employs superposition coding (SC) at the transmitter side to superimpose the desired signal of multiple users using power domain which generates inter user interference (IUI). Successive interference cancellation (SIC) is applied at the receiver side to eliminate the IUI and decode the desired transmitted signal. Application of multiple antenna technologies to NOMA further enhances the performance of NOMA system [15–17]. Sum-rate maximization (SRM) is an indispensable task in signal design for communication, and particularly for NOMA systems. We examine the problem of weighted sum-rate maximization (WSRM) for multicell MIMO-NOMA downlink system with imperfect channel state information at the transmitter (CSIT). The examined WSRM problem is acknowledged as NP-hard problem.

Distinct approaches for WSRM problem have been proposed in literature [18–23] for the perfect CSI at the BSs. For instance, SRM problem was formulated in [18] for a two user MIMO-NOMA system where the authors established a beamforming design based on singular value decomposition (SVD) and power allocation scheme to maximize the sum-rate. Authors in [19] studied the SRM problem for a downlink NOMA system where they proposed a dynamic resource allocation algorithm to show the effectiveness

* Corresponding author.

E-mail addresses: sunilkcsss@jbnu.ac.kr (S. Chinnadurai), poongundran@jbnu.ac.kr (P. Selvaprabhu), latifsarker@jbnu.ac.kr (A.L. Sarker), haihan@jbnu.ac.kr (H. Hai), sinder@live.cn (W. Duan), moonho@jbnu.ac.kr (M.H. Lee).

of NOMA over OFDMA scheme. In [20], a user selection and power schedule algorithm were proposed to maximize the sum-rate of downlink single cell NOMA system with zero forcing beamforming (ZFBF) scheme. Authors in [21] proposed two low complexity sub optimal power allocation schemes to maximize the sum-rate for a subcarrier based NOMA system. In [22], authors proposed a NOMA scheme where random beamforming (RABF) is employed to achieve the better sum-rate than the conventional OMA scheme and authors in [23] focus on the SRM problem for a downlink MISO-NOMA system to enhance the sum-rate. However, the works mentioned above [18–23] assume perfect CSIT which is very difficult to obtain in practice due to the inaccurate channel estimation, deficient channel reciprocity, feedback quantization, delays and so on. Thus, it is meaningful to deal with the imperfect CSI in the problem formulation. Imperfect CSI can be formed either via statistical distribution [24,25] or the deterministic distribution [26–28], where the CSI errors lie in a bounded uncertainty region.

In this paper, we especially consider a singular value uncertainty model (SVUM) [26] to form the CSI errors and robust design of the beamforming matrix is taken into account to solve the worst-case WSRM problem. Few relevant results prevail in the literature which consider imperfect CSIT. In particular, authors in [29] examined the performance of a multiuser (MU) single Cell (SC)-NOMA system with distinct channel uncertainty models established on imperfect CSI and statistical CSI at the transmitter. Ergodic sum rate and outage probability for MU SC-NOMA system with statistical CSI were studied in [30] assuming fixed power allocation. Considering statistical CSIT, optimal power allocation schemes were proposed in [31] to solve the SRM problem with the transmit power constraint for a two user MIMO-NOMA system. An efficient power allocation scheme was introduced in [32] to achieve the maximum fairness between two users in a SISO-NOMA system under statistical CSIT. A MU MIMO-NOMA scheme was proposed in [33] with limited feedback at the transmitter. Authors in [34] investigated the impact of user pairing by analyzing the sum-rate performance of a two user SISO-NOMA system where a fixed power allocation scheme is employed among NOMA users. Although there exists enormous interest in WSRM problem, most of the authors considered the problem only in SC-NOMA system with the assumption of statistical CSIT. So, it largely remains unsolved in typical scenarios of interest. For instance, a robust beamforming design for a multicell MIMO-NOMA system with imperfect CSIT due to the deterministic distribution that achieves capacity in the downlink is yet to be characterized.

In light of the above, the major contributions of this paper can be encapsulated as follows.

- WSRM problem is formulated subject to the total transmit power constraint at the BS. We have considered SVUM to include CSI errors. The motivation behind using SVUM is that they bound the CSI errors to produce a feasible worst-case design. Generally, it is very difficult to resolve this NP-hard problem.
- A robust beamforming design is investigated to examine the WSRM problem in the downlink multicell MIMO-NOMA system. In particular, an efficient iterative algorithm which establishes on the majorization minimization (MM) technique [36–38] is proposed to solve the worst-case WSRM problem with SVUM. With the proposed iterative algorithm, the optimal beamforming (BF) matrix can be easily found which not only increases the system performance but also reduces the inter cell interference (ICI).
- We also propose a joint user clustering and power allocation (JUCPA) algorithm to mitigate the inter user interference (IUI) and the inter cluster interference (ICRI) that exists in the objective function of WSRM problem. The JUCPA algorithm utilizes

minimum distance factor (MDF) and the channel correlation to cluster the users effectively which in turn improves the system performance.

- Numerical results confirm that a significant improvement in the sum-rate is achieved by using the proposed NOMA scheme (JUCPA and IMM algorithm) as compared with the ZFBF scheme proposed in [20], the RABF scheme proposed in [22] and the conventional OMA scheme in [35].

The rest of this paper is organized as follows. Section II describes the considered system model for the downlink of a multicell MIMO-NOMA system. Weighted sum-rate maximization (WSRM) problem is formulated with SVUM in section III. Joint user clustering and power allocation algorithm is proposed in section IV. Robust beamforming design with SVUM is discussed in section V. Comprehensive numerical results are presented to show the excellent performance of our proposed scheme for multicell MIMO-NOMA system in Section VI, and Section VII concludes this paper.

Notations: \mathbf{A}^T denote the transpose of a matrix \mathbf{A} . An $N \times N$ identity matrix is denoted by \mathbf{I}_N . $E(\cdot)$ and $tr(\cdot)$ stands for the statistical expectation and trace of a matrix respectively. $\hat{\mathbf{H}}$ denotes an estimate of \mathbf{H} . All logarithms are in base two unless specified. $I(A;B)$ is mutual information between the random variables A and B . The circularly symmetric complex Gaussian distribution with mean A and variance B is denoted by $\mathcal{CN}(A,B)$. $\mathbf{X} \succeq 0$ and $\mathbf{X} \succ 0$ indicates that the matrix \mathbf{X} is positive semi definite and positive definite respectively. The set of all $A \times B$ complex matrices is denoted by $\mathbb{C}^{A \times B}$. The operation $(\cdot)^\dagger$ denotes hermitian transpose of a matrix or vector.

2. System model

We study the downlink transmission of a multicell MIMO-NOMA system where in each cell, BS p equipped with $n_{B,p}$ antennas serves M clusters as exemplified in Fig. 1. Each cluster m has 2 users which are served by one antenna from the base station (BS). Considering the NOMA scheme from [5], BS aggregates the desired message of 2 users in m^{th} cluster and transmit the combined signal with the same beamforming vector but with different power allocation coefficients at the same time and frequency slot via power domain NOMA. Each k^{th} user will obtain its desired signal and the signal predestined for the other user present in the m^{th} cluster. Therefore, successive interference cancellation (SIC) is employed at the receiver to detect its desired signal. An overview of the transmitter (Tx) and receiver (Rx) side of the considered MIMO-NOMA downlink system is epitomized in Fig. 2. We categorize the two users present in each cluster as cell center (CC) users and cell edge (CE) users based on the efficient joint user clustering and power allocation (JUCPA) algorithm proposed in section IV. CC and CE users are considered as strong and weak users respectively. BS allocates more power to CE users, since it needs more power to decode its desired message. Furthermore, only CC users which are close to the BS implements SIC to decode its desired signal by treating the other user's signal as noise. This is due to the fact that the large amount of transmission power will be required to implement SIC at both receivers.

A MIMO-NOMA system consisting of N_M MSs, N_B BSs, M clusters and N cells are considered. The signal $E_{m,n}$ for m^{th} cluster in n^{th} cell is evenly assigned as $\{1, 2, 3, \dots, 2^{cR_{m,n}}\}$, where $R_{m,n}$ represents the information rate of cluster m in bits per channel use (c.u.) and c is blocklength. Each MS k is provided with $n_{M,k}$ antennas and each BS p is provided with $n_{B,p}$ antennas for $\{k = 1, 2, 3, \dots, N_M\}$ and $\{p = 1, 2, 3, \dots, N_B\}$ respectively. We specify $n_B = \sum_{p=1}^{N_B} n_{B,p}$ as the

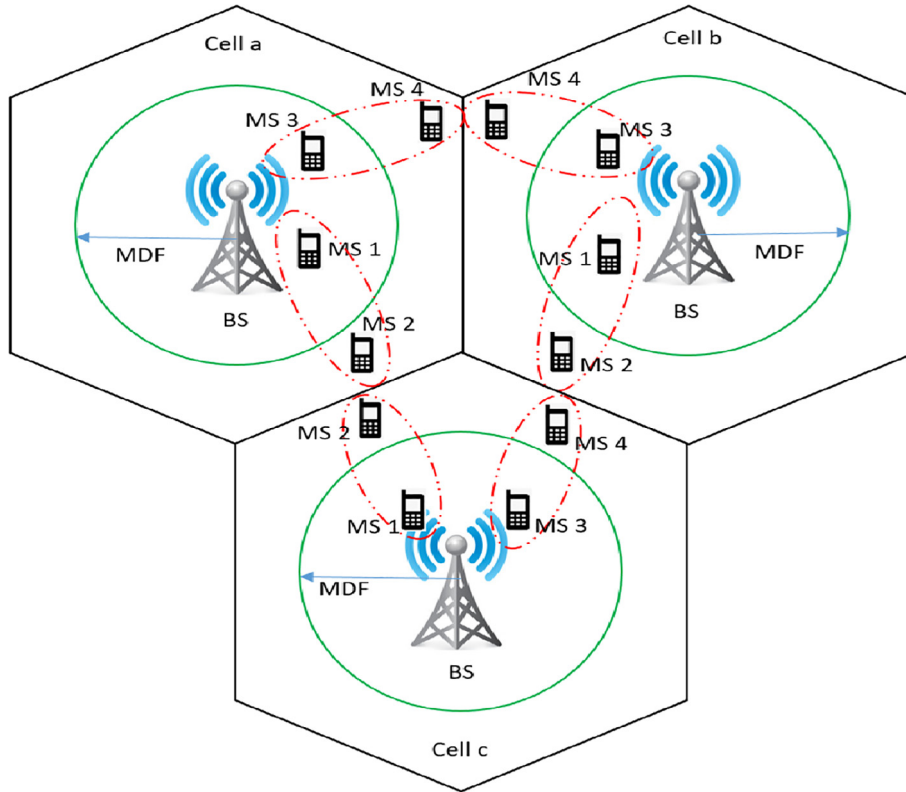


Fig. 1. Multicell MIMO-NOMA downlink system.

total number of transmitting antennas and $n_M = \sum_{k=1}^{N_M} n_{M,k}$ as the total number of receive antennas. We also specify the sets $\mathcal{N}_B = \{1, 2, 3, \dots, N_B\}$, $\mathcal{N} = \{1, 2, 3, \dots, N\}$, $\mathcal{M} = \{1, 2, 3, \dots, M\}$ and $\mathcal{N}_M = \{1, 2, 3, \dots, N_M\}$. Each signal $E_{m,n}$ for m^{th} cluster is predetermined for a given channel use and we have $r_{m,n} \leq n_{M,k}$ where $m \in \mathcal{M}$ and $n \in \mathcal{N}$. We assume $n_{M,m}$ and $n_{M,n}$ as the number of MS antennas present in each cluster and cell respectively. The superimposed signal of CC and CE users belonging to the m^{th} cluster in n^{th} cell is given as

$$E_{m,n} = \sqrt{P_{1,m,n}}S_{1,m,n} + \sqrt{P_{2,m,n}}S_{2,m,n}, \quad (1)$$

where $S_{1,m,n}$ and $S_{2,m,n}$ are the desired signal for CC users and CE users respectively. The power allocated to m^{th} cluster is expressed below as

$$P_{1,m,n} + P_{2,m,n} = 1, \quad (2)$$

where $P_{1,m,n}$ and $P_{2,m,n}$ represents the power allocated to CC and CE user respectively. The signals $E_{1,n}, E_{2,n}, E_{3,n}, \dots, E_{M,n}$ goes through the precoding process which usually restricts the interference between the data streams predetermined for the same cluster and for the different clusters. Encoded signals can be precoded via both linear and non-linear precoding to handle the interference across the clusters and also amid the data streams for same cluster. Here, we consider linear precoding which is given as

$$\mathbf{W} = [W_{1,n}, W_{2,n}, W_{3,n}, \dots, W_{M,n}], \quad (3)$$

where $m \in \mathcal{M}$ and $W_{m,n} \in \mathbb{C}^{1 \times n_{M,m}}$ represents the beamforming vector corresponding to cluster m . The transmitted signal vector from n_B antennas are given as

$$\mathbf{x} = \mathbf{W}\mathbf{E}, \quad (4)$$

where $\mathbf{E} \in \mathbb{C}^{n_M \times n_{M,k}}$ represents the encoded signals, $\mathbf{W} \in \mathbb{C}^{n_B \times n_M}$ is the beamforming matrix and $\mathbf{E} = [E_{1,n}^T, E_{2,n}^T, \dots, E_{M,n}^T]^T$. The transmit power constraints for each BS is given by

$$\text{tr}\{E(x_p x_p^H)\} \leq P_p, \quad p \in \mathcal{N}_B, \quad (5)$$

where P_p is the maximum power transmitted at the BS. The signal vector received by m^{th} cluster in n^{th} cell is given as

$$\mathbf{y}_{m,n} = \mathbf{H}_{m,n}\mathbf{x} + \mathbf{z}_{m,n}, \quad (6)$$

where $\mathbf{x} = [x_1^T, x_2^T, \dots, x_{N_B}^T]^T$ and $\mathbf{z}_{m,n}$ is the additive white gaussian noise (AWGN) vector with $\mathcal{CN}(0, \sigma_{m,n}^2)$. The over all channel matrix for all the clusters can be expressed as follows

$$\mathbf{H} = [\mathbf{H}_{1,n}, \mathbf{H}_{2,n}, \mathbf{H}_{3,n}, \dots, \mathbf{H}_{M,n}], \quad (7)$$

where $\mathbf{H} \in \mathbb{C}^{n_M \times n_B}$. The channel matrix corresponding to m^{th} cluster in n^{th} cell is written as

$$\mathbf{H}_{m,n} = [h_{1,m,n}, h_{2,m,n}]^T, \quad (8)$$

where $h_{k,m,n} \in \mathbb{C}^{n_{B,p} \times n_{M,k}}$ represents the channel vector from BS p to user k in m^{th} cluster. The received signal by the m^{th} cluster in n^{th} cell is given as

$$\mathbf{y}_{m,n} = \mathbf{y}_{1,m,n} + \mathbf{y}_{2,m,n}, \quad (9)$$

where $\mathbf{y}_{1,m,n}$ and $\mathbf{y}_{2,m,n}$ are the received signal by CC and CE user respectively which are expressed in Eqs. (10) and (11) respectively.

$$\mathbf{y}_{1,m,n} = \mathbf{h}_{1,m,n}^T \mathbf{W}_{m,n} \sqrt{P_{1,m,n}} S_{1,m,n} + \sum_{j=1, j \neq m}^M \mathbf{h}_{1,m,n}^T \mathbf{W}_{j,n} E_{j,n} + \mathbf{z}_{1,m,n}, \quad (10)$$

where $E_{j,n} = \sqrt{P_{1,j,n}}S_{1,j,n} + \sqrt{P_{2,j,n}}S_{2,j,n}$ and $\mathbf{z}_{1,m,n}$ is the AWGN noise with $\mathcal{CN}(0, \sigma_{1,m,n}^2)$. In (10), the first term represents the desired sig-

nal to CC user and the second term is due to the interference from other clusters present in the same cell which we call as the inter cluster interference (ICRI). Inter user interference (IUI) that occurs due to CE user present in the same cluster is cancelled due to the implementation of SIC at the CC user.

$$y_{2,m,n} = h_{2,m,n}^T W_{m,n} \sqrt{P_{2,m,n}} S_{2,m,n} + \Xi + \Pi + \sum_{c \in \mathcal{N} \setminus n} \sum_{m=1}^M g_{2,m,c}^T W_{m,c} E_{m,c} + z_{2,m,n}, \quad (11)$$

where $\Xi = h_{2,m,n}^T W_{m,n} \sqrt{P_{1,m,n}} S_{1,m,n}$, $\Pi = \sum_{j=1, j \neq m}^M h_{2,m,n}^T W_{j,n} E_{j,n}$ and $z_{2,m,n}$ is the AWGN noise vector with $\mathcal{CN}(0, \sigma_{2,m,n}^2)$. $g_{2,m,c}^T$ represents the interfering channel vector (from other cell) to the CE user present at the m^{th} cluster of n^{th} cell. In (11), the first term is the desired signal to CE user and the second term is the interference from CC user present in the same cluster which we call it as inter user interference (IUI). The third term is the ICRI and the fourth term is due to the interference from the CE users present in other cells which is called as inter cell interference (ICI). The achievable downlink rate of the transmission from BS to m^{th} cluster is the mutual information between the unknown transmitted signal $E_{m,n}$ and the observed received signal $y_{m,n}$ is obtained as

$$R_{m,n} = I(E_{m,n}; y_{m,n}) = (R_{1,m,n} + R_{2,m,n}), \quad (12)$$

where $R_{1,m,n}$ and $R_{2,m,n}$ are the achievable downlink rates by the CC and CE users respectively. The achievable rates for CC user with perfect and imperfect SIC receiver are given in Eqs. (13) and (14) respectively.

$$R_{1,m,n} = \log_2 \left(\mathbf{1} + \frac{P_{1,m,n} |h_{1,m,n}^T W_{m,n}|^2}{\sum_{j=1, j \neq m}^M |h_{1,m,n}^T W_{j,n}|^2 + \sigma_{1,m,n}^2} \right). \quad (13)$$

$$R_{1,m,n} = \log_2 \left(\mathbf{1} + \frac{P_{1,m,n} |h_{1,m,n}^T W_{m,n}|^2}{\sum_{j=1, j \neq m}^M |h_{1,m,n}^T W_{j,n}|^2 + \mu P_{2,m,n} |h_{1,m,n}^T W_{m,n}|^2 + \sigma_{1,m,n}^2} \right). \quad (14)$$

$$R_{2,m,n} = \log_2 \left(\mathbf{1} + \frac{P_{2,m,n} |h_{2,m,n}^T W_{m,n}|^2}{P_{1,m,n} |h_{2,m,n}^T W_{m,n}|^2 + \sum_{j=1, j \neq m}^M |h_{2,m,n}^T W_{j,n}|^2 + \sum_{c \in \mathcal{N} \setminus n} \sum_{m=1}^M |g_{2,m,c}^T W_{m,c}|^2 + \sigma_{2,m,n}^2} \right). \quad (15)$$

Imperfect successive interference cancellation (SIC) is considered at CC user to provide a more realistic analysis as compared to the perfect SIC receiver given in Eq. (13). SIC error μ at the CC user is mainly caused because of the less difference in the channel gains between the paired users and also due to the channel uncertainty at the transmitter. SIC error can cause huge performance degradation when many users are paired. However in our proposed scheme, SIC error will have a less impact on the sum rate performance since we consider only 2 users per cluster for each cell. The achievable rate of CE user given in Eq. (15) does not get affected due to SIC, since it is employed only at the CC user. The weighted sum-rate for all clusters are expressed as

$$R_{\text{sum}} = \sum_{n \in \mathcal{N}} \sum_{m \in \mathcal{M}} B_{m,n} R_{m,n}, \quad (16)$$

where $B_{m,n} \geq 0$ are fixed weights for each cluster. These weights emulate the user priority which are generally chosen by the network operators based on the fairness and network throughput.

3. Problem formulation

In this section, we formulate the WSRM problem for MIMO-NOMA downlink system with imperfect CSI at the BS. Here, we consider SVUM or multiplicative uncertainty model to include CSI errors [26]. Multiplicative uncertainty model (MUM) represents the uncertainty of a true frequency response where the robust capacity is defined as the max-min of the mutual information rate in which the maximum is over all the power spectral densities (PSD) of signal transmitted with constrained power and the minimum is over the frequency responses from the multiplicative uncertainty set [43]. Multiplicative channel matrix is defined as the multiplication of nominal channel matrix and the unknown (bounded) channel uncertainty matrix which is shown in Fig. 3. Generally, it is very difficult to obtain the perfect CSIT in practice. So, robustness has been demanding issue which can be addressed by two popular designs i.e. stochastic and deterministic approach. In stochastic uncertainty model (SUM), CSI errors are unbounded and assume gaussian random variables with the known statistical distributions

$$\mathbf{H}_{m,n} = \hat{\mathbf{H}}_{m,n} (\mathbf{I} + \Delta_{m,n}), \quad (17)$$

where $\Delta_{m,n} \in \mathcal{CN}(0, D)$ are CSI errors with zero mean and covariance D [26,27]. In deterministic uncertainty model (DUM), the CSI errors are assumed to be deterministically bounded by a known set (possible values) but its actual value is unknown to the transmitter. In addition, bounded CSI errors can be taken into account by various uncertainty models like ellipsoidal uncertainty, singular value uncertainty, arbitrary normed uncertainty, spherical uncertainty, etc. For example, ellipsoidal uncertainty model (EUM) can also be considered to include CSI error where the uncertainty region can be bounded as follows

$$\mathcal{H}_{m,n} = \{ \hat{\mathbf{H}}_{m,n} + \psi_{m,n} | \text{tr}(\psi_{m,n} \mathbf{L} \psi_{m,n}^\dagger) \leq \varepsilon^2 \}, \quad (18)$$

where $\mathbf{L} \geq 0$ is a given matrix which represents the shape of the region and ε^2 manages the size of the ellipsoidal region [28]. As mentioned before, we consider singular value uncertainty model (SVUM) to include CSI errors since its induced norm constraint channel matrix helps to analyze the system capacity of MIMO systems [26] which are robust to channel uncertainties. SVUM also helps to determine the achievable rate for different sizes of the uncertainty region. The channel matrix $\mathbf{H}_{m,n}$ for each cluster m using SVUM is given as

$$\mathbf{H}_{m,n} = \hat{\mathbf{H}}_{m,n} (\mathbf{I} + \Delta_{m,n}), \quad (19)$$

where the matrix $\hat{\mathbf{H}}_{m,n}$ is the estimate of channel $\mathbf{H}_{m,n}$ and $\Delta_{m,n} \in \mathbb{C}^{n_B \times n_B}$ represent multiplicative uncertainty matrix whose appropriate bounds are given as

$$\begin{aligned} \mathbf{H}_{m,n} &\in \mathcal{S}_{\mathbf{H}_{m,n}} = \{\mathbf{H}_{m,n} : \|\Delta_{m,n}\|_2 \leq \epsilon_{m,n}\}, \\ \|\Delta_{m,n}\|_2 &= \sigma_{\max}(\Delta_{m,n}) \leq \epsilon_{m,n} < 1, \end{aligned} \quad (20)$$

where $\sigma_{\max}(\Delta_{m,n})$ represents the largest singular value of matrix $\Delta_{m,n}$, $\epsilon_{m,n}$ determines the channel error bound and $\mathcal{S}_{\mathbf{H}_{m,n}}$ is the multiplicative uncertainty set. The WSRM problem for SVUM is formulated as follows

$$\begin{aligned} \max_{\mathbf{W} \geq 0} \quad & \min_{\mathbf{H}_{m,n} \in \mathcal{S}_{\mathbf{H}_{m,n}}} \sum_{m=1}^M B_{m,n} f_{m,n}(\mathbf{W}) \\ \text{s.t.} \quad & \text{tr}(\mathbf{W}\mathbf{W}^T) \leq P_p, \end{aligned} \quad (21)$$

where $f_{m,n}(\mathbf{W}) \triangleq R_{m,n}$, $m \in \mathcal{M}$, $p \in \mathcal{N}_B$ and uncertainty bound for $\Delta_{m,n}$ was already given in Eq. (20). The objective function in Eq. (21) maximizes the worst-case weighted sum-rate over all the feasible uncertainty matrices $\Delta_{m,n}$ subject to the transmit power constraint. By employing Theorem 1 from [26], result of the following problem given in Eq. (22) is obtained

$$\min_{\mathbf{H}_{m,n} \in \mathcal{S}_{\mathbf{H}_{m,n}}} f_{m,n}(\mathbf{W}) \quad (22)$$

when $\Delta_{m,n} = -\epsilon_{m,n}\mathbf{I}$. Replacing the value of $\Delta_{m,n}$ in (19), we can express the channel matrix as

$$\mathbf{H}_{m,n} = \hat{\mathbf{H}}_{m,n}(\mathbf{I} - \epsilon_{m,n}\mathbf{I}) = \hat{\mathbf{H}}_{m,n}(1 - \epsilon_{m,n}), \quad (23)$$

where $n \in \mathcal{N}$. Substituting (23) in (8), we get

$$\mathbf{H}_{m,n} = [\hat{h}_{1,m,n}(1 - \epsilon_{m,n}), \hat{h}_{2,m,n}(1 - \epsilon_{m,n})]^T, \quad (24)$$

with $\hat{h}_{k,m,n} \in \mathbb{C}^{n_{M,k} \times n_{B,p}}$ represents the estimate of channel vector from BS p to MS k in m^{th} cluster. As seen in Eq. (24), there are two users present in each cluster which will be selected by the JUCPA algorithm proposed in the next section. All through this paper, we explicitly the estimated channel vector as \hat{h}_k instead of $\hat{h}_{k,m,n}^T(1 - \epsilon_{m,n})$ for simplicity.

4. Proposed joint user clustering and power allocation (JUCPA) algorithm

The proposed JUCPA algorithm aims to mitigate the inter user interference (IUI) and inter cluster interference (ICRI) present in the original problem formulated in Eq. (21). As mentioned in the previous section, each cluster m has two users (CC and CE) which are positioned at \hat{h}_1 and \hat{h}_2 . The mean channel gains are expressed as $\hat{h}_1^{-\gamma}$ and $\hat{h}_2^{-\gamma}$ for CC (user 1) and CE (user 2) user respectively, where γ is the path loss exponent. We derive the minimum distance factor (MDF) and consider it as a metric to differentiate the users present in each cell into CC and CE user using the condition [35] given below

$$R_k^{(NOMA)} > R_k^{(OMA)}, \forall k \in \mathcal{N}_M, \quad (25)$$

where

$$R_1^{(NOMA)} = \log_2(1 + P_{1,m,n}P\hat{h}_1^{-\gamma}). \quad (26)$$

$$R_2^{(NOMA)} = \log_2\left(1 + \frac{P_{2,m,n}P\hat{h}_2^{-\gamma}}{P_{1,m,n}P\hat{h}_2^{-\gamma} + 1}\right). \quad (27)$$

$$R_k^{(OMA)} = \frac{1}{2} \log_2(1 + P\hat{h}_k^{-\gamma}), \forall k = 1, 2. \quad (28)$$

Considering Eqs. (26) and (28) in (25), we get

$$MDF = \left(\frac{1 - 2P_{1,m,n}}{P_{1,m,n}^2 P}\right)^{\frac{1}{\gamma}}, \quad (29)$$

where $\hat{h}_1 \leq MDF$ and $\hat{h}_2 > MDF$, i.e. CC users will be present within MDF region and CE users will be present beyond the MDF region. $P_{1,m,n}$ indicates the power allocation coefficient for CC user and $P = P_p/\sigma_{m,n}^2$ is the transmit SNR. We assume $\sigma_{1,m,n}^2 = \sigma_{2,m,n}^2 = \sigma_{m,n}^2$ for simplicity. The proof for Eq. (29) is derived below by considering $k = 1$ in Eq. (24) as

$$\begin{aligned} (1 + P_{1,m,n}P\hat{h}_1^{-\gamma}) &> (1 + P\hat{h}_1^{-\gamma})^{1/2}, \\ (1 + P_{1,m,n}P\hat{h}_1^{-\gamma})^2 &> (1 + P\hat{h}_1^{-\gamma})^1, \\ P_{1,m,n}^2 P\hat{h}_1^{-\gamma} + 2P_{1,m,n} &> 1, \\ \hat{h}_1 &\leq \left(\frac{1 - 2P_{1,m,n}}{P_{1,m,n}^2 P}\right)^{\frac{1}{\gamma}}. \end{aligned} \quad (30)$$

Similarly, we can also derive the MDF for CE user by assuming $k = 2$ in Eq. (27). We follow the fixed transmit power allocation (FTPA) scheme as in [30]. User fairness of the proposed JUCPA algorithm in multicell MIMO-NOMA downlink system is examined based on user fairness index embraced from [39]. User fairness between the CC and CE user in a cluster is given as follows

$$\Upsilon = \frac{(R_{1,m,n} + R_{2,m,n})^2}{2(R_{1,m,n}^2 + R_{2,m,n}^2)} \forall m \in \mathcal{M}, \quad (31)$$

where $R_{1,m,n}$ and $R_{2,m,n}$ are given in Eqs. (13) and (15) respectively. The value of Υ is compassed between 0 and 1 while the largest value attained by leveling the user's (CC and CE) achievable rates. Proportion fairness (PF) algorithm has been used in [40,41] to schedule the user set P_{opt} which is given as follows.

$$P_{opt} = \arg \max_{P \subseteq K} \sum_{k \in P} \frac{R_{k|P}(t)}{C_k(t)} \quad (32)$$

where $R_{k|P}(t)$ and $C_k(t)$ is the instantaneous achievable data rate and average user throughput of user k at time instant t respectively. K and P represents the set of user candidates and scheduled user set respectively. Although PF algorithm achieves the satisfying tradeoff between the user fairness and the user throughput, it is not suitable for some of the real time applications since it does not provide sufficient quality of service (QoS) requirement for users with delay constraint. So, PF scheduler struggles to minimize the interference in the considered multicellular network. Moreover, PF algorithm does not balance the load in the heterogeneous cellular network since it schedules the cell center (CC) users twice as much as cell edge (CE) users. In order to achieve the considerable user fairness, PF scheduler allocates larger weights to CE users which in turn degrades the sum rate performance of the over all system. The proposed JUCPA algorithm not only overcomes the above problems encountered by PF algorithm but also increases the sum-rate of the MIMO-NOMA system. Algorithm 1 summarizes the steps of proposed joint user clustering and power allocation (JUCPA) algorithm. In step 1, users are split into two categories i.e., CC and CE based on MDF given in (29) to reduce IUI between users in the same cluster. Users are clustered in step 2 based on the maximum correlation between the CC and CE user, since it guarantees to mitigate the ICRI. In step 3, we remove the clustered users (paired users in step 2) from the CC and CE user sets. Repeat step 2 and step 3 until CC or CE user set is empty. The unclustered users receives their desired signal via conventional OMA scheme in step 4 and algorithm exits in step 5.

Algorithm 1. Proposed JUCPA algorithm

Step1. Initialization and splitting: Initialize

$i = 1, m = 1, D = \{\hat{h}_1, \hat{h}_2, \dots, \hat{h}_K\}, \mathcal{I} = \{1, 2, 3, \dots, I\}$ and $\mathcal{J} = \{1, 2, 3, \dots, J\}$.

$$D = \begin{cases} CC, & \text{if } \hat{h}_k \leq MDF \\ CE, & \text{else} \end{cases}$$

where D is expressed as the set of all user's CSI feedback of n^{th} cell. CC and CE user sets are categorized in (33) and (34) respectively based on the MDF given in Eq. (29).

$$CC = \{\hat{h}_1, \hat{h}_2, \dots, \hat{h}_i\}, \tag{33}$$

$$CE = \{\hat{h}_1, \hat{h}_2, \dots, \hat{h}_j\}, \tag{34}$$

where i and j represents the CC and CE user index respectively ($i \in \mathcal{I}$ and $j \in \mathcal{J}$).

Step2. Correlation: Find the correlation between the user i from CC and all the j users present in CE given in Eq. (34)

$$\hat{h}_j^* = \underset{h_j \in CE}{\operatorname{argmax}} \operatorname{Corr}(\hat{h}_i, \hat{h}_j), \tag{35}$$

where

$$\operatorname{Corr}(\hat{h}_i, \hat{h}_j) = \frac{|\hat{h}_i \hat{h}_j^*|}{|\hat{h}_i| |\hat{h}_j|}. \tag{36}$$

Step3. Remove and Repeat: Remove the selected users

$\mathbf{H}_{m,n} = [\hat{h}_i, \hat{h}_j]$ from (33) and (34). Save them in $\mathbf{H} = [\mathbf{H}_{1,n}, \mathbf{H}_{2,n}, \dots, \mathbf{H}_{M,n}]$, where m represents the cluster index.

$$\begin{aligned} CC &= CC - \hat{h}_i, \\ CE &= CE - \hat{h}_j, \end{aligned} \tag{37}$$

Case1 : $CC \neq \{\}$ and $CE \neq \{\}$:

if $i < I$,
 $i \leftarrow i + 1; m \leftarrow m + 1$;
 repeat Step 2 and step 3.
 else
 go to step 5.

Case2 : $CE = \{\}$ or $CC = \{\}$:

if $i < I$,
 go to Step 4. (38)

Step4. Unclustered Users: Balance users present in (34) will be serviced based on the conventional OMA scheme.

Step5. Exit: Stop the Algorithm.

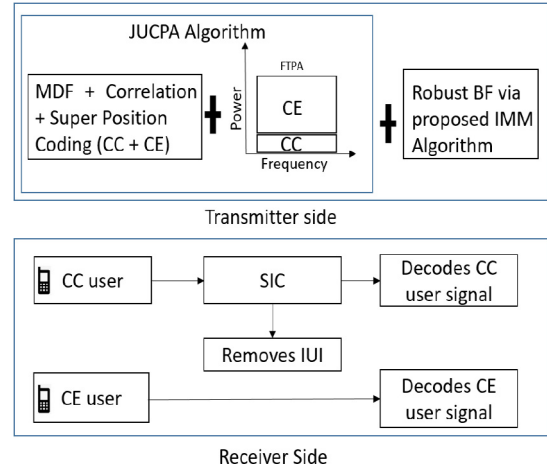


Fig. 2. Transmitter and Receiver of MIMO-NOMA downlink system.

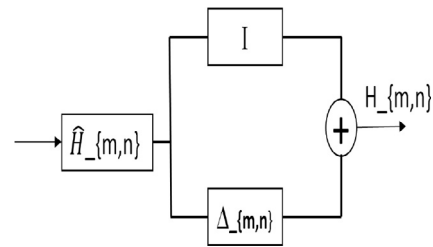


Fig. 3. Multiplicative uncertainty model.

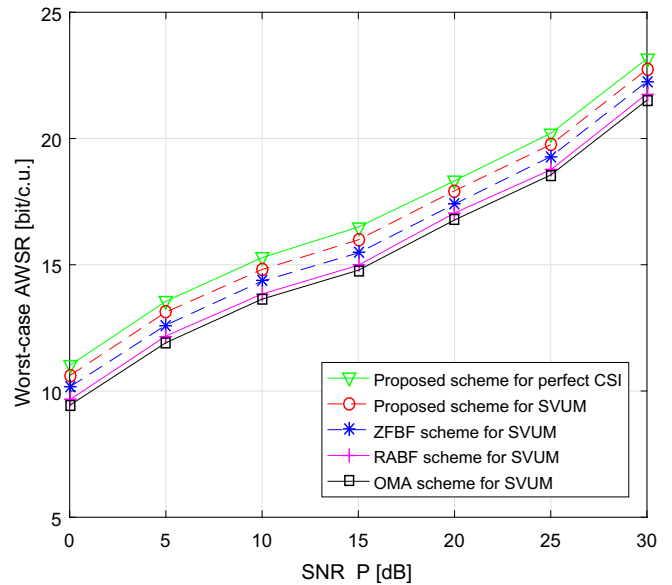


Fig. 4. Worst-case AWSR versus SNR with perfect SIC for $\hat{h}_1 = 40$ m, $\hat{h}_2 = 120$ m and $P_{2,m,n} = 0.9$.

where $R_{1,m,n}(\mathbf{W})$ and $R_{2,m,n}(\mathbf{W})$ are the achievable rates for the CC and CE users given in Eqs. (40) and (41) respectively.

$$R_{1,m,n}(\mathbf{W}) = \log_2 \left(\mathbf{1} + \frac{P_{1,m,n} \hat{h}_1 (\mathbf{W}\mathbf{W}^H)^{-1} \hat{h}_1^*}{\Phi + \sigma_{1,m,n}^2} \right), \tag{40}$$

5. Robust beamforming design with SVUM

In this section, we propose an iterative MM algorithm to find the transmit beamforming vector for all the clusters (paired users) formed by JUCPA algorithm. The achievable rate for cluster m in the presence of bounded uncertainties (given in Eq. (20) for SVUM) at the BS is written as

$$f_{m,n}(\mathbf{W}) \triangleq R_{1,m,n}(\mathbf{W}) + R_{2,m,n}(\mathbf{W}), \tag{39}$$

$$R_{2,m,n}(W) = \log_2 \left(\mathbf{1} + \frac{P_{2,m,n} \hat{h}_2(\mathbf{W}\mathbf{W}^\dagger) \hat{h}_2^\dagger}{P_{1,m,n} \hat{h}_2(\mathbf{W}\mathbf{W}^\dagger) \hat{h}_2^\dagger + \sum_{j=1, j \neq m}^M \hat{h}_2(\mathbf{W}_j \mathbf{W}_j^\dagger) \hat{h}_2^\dagger + \sum_{c \in \mathcal{N} \setminus \mathcal{N}} \sum_{m=1}^M \hat{g}_{2,m,c}(\mathbf{W}\mathbf{W}^\dagger) \hat{g}_{2,m,c}^\dagger + \sigma_{2,m,n}^2} \right), \quad (41)$$

where $\Phi = \sum_{j=1, j \neq m}^M \hat{h}_2(\mathbf{W}_j \mathbf{W}_j^\dagger) \hat{h}_2^\dagger$ and $\hat{g}_{2,m,n} \triangleq \hat{g}_{2,m,n}^T (1 - \epsilon_{m,n})$. The beamforming matrix W is not positive semi definite and the constraints present in Eq. (21) are quadratic. So, the over all problem becomes non-convex which is called as non-convex quadratically constrained quadratic problem (QCQP). We introduce a new variable by defining the transmit covariance matrices $\mathbf{G}_{m,n} \triangleq W_{m,n} W_{m,n}^\dagger \geq 0$ in the below equation,

$$\begin{aligned} \max_{\{\mathbf{G}_{m,n}\}_{m=1}^M} & \sum_{m=1}^M B_{m,n} f_{m,n}(\{\mathbf{G}_{m,n}\}_{m=1}^M) \\ \text{s.t.} & \quad \text{tr}(\mathbf{G}_{m,n}) \leq P_p, \text{rank}\{\mathbf{G}_{m,n}\} = 1 \end{aligned} \quad (42)$$

Semi definite programming (SDP) approach is employed here to deal the optimization problem over positive symmetric semidefinite matrix with linear constraint and cost functions. In addition, we also implement the semi definite relaxation (SDR) approach [44] to relax the rank constraint i.e. $\text{rank}\{\mathbf{G}_{m,n}\} = 1$ by replacing with the semi definite matrix $G \geq 0$. Considering the above observations, the problem given in Eq. (21) can be equivalently reformulated as follows

$$\begin{aligned} \max_{\{\mathbf{G}_{m,n} \geq 0\}_{m=1}^M} & \sum_{m=1}^M B_{m,n} f_{m,n}(\{\mathbf{G}_{m,n}\}_{m=1}^M) \\ \text{s.t.} & \quad \text{tr}(\mathbf{G}_{m,n}) \leq P_p, \end{aligned} \quad (43)$$

where

$$f_{m,n}(\{\mathbf{G}_{m,n}\}_{m=1}^M) \triangleq R_{1,m,n}(\{\mathbf{G}_{m,n}\}_{m=1}^M) + R_{2,m,n}(\{\mathbf{G}_{m,n}\}_{m=1}^M), \quad (44)$$

where the first and second term in (44) are given in Eqs. (45) and (46) respectively.

$$R_{1,m,n}(\{\mathbf{G}_{m,n}\}_{m=1}^M) = \log_2 \left(\mathbf{1} + \frac{P_{1,m,n} \hat{h}_1(\mathbf{G}_{m,n}) \hat{h}_1^\dagger}{\Omega + \sigma_{1,m,n}^2} \right), \quad (45)$$

$$\begin{aligned} R_{2,m,n}(\{\mathbf{G}_{m,n}\}_{m=1}^M) \\ = \log_2 \left(\mathbf{1} + \frac{P_{2,m,n} \hat{h}_2(\mathbf{G}_{m,n}) \hat{h}_2^\dagger}{P_{1,m,n} \hat{h}_2(\mathbf{G}_{m,n}) \hat{h}_2^\dagger + \Theta + \sum_{c \in \mathcal{N} \setminus \mathcal{N}} \sum_{m=1}^M \hat{g}_{2,m,c}(\mathbf{G}_{m,c}) \hat{g}_{2,m,c}^\dagger + \sigma_{2,m,n}^2} \right), \end{aligned} \quad (46)$$

where $\Omega = \sum_{j=1, j \neq m}^M \hat{h}_{1,m,n}(\mathbf{W}_j \mathbf{W}_j^\dagger) \hat{h}_{1,m,n}^\dagger$ is due to the ICRI. In Eq. (46), the first and third term in the denominator represents the IUI and ICI respectively. The second term in (46) represents the ICRI which is given by $\Theta = \sum_{j=1, j \neq m}^M \hat{h}_2(\mathbf{G}_j) \hat{h}_2^\dagger$. The problem mentioned in (43) is still not straightforward to determine due to the non-convexity of the objective function. Furthermore, objective function given in (43) falls under difference of convex (DC) problem. Several approaches like Majorization minimization (MM) algorithm, alternating optimization (AO) algorithm are available in [36–38,42] to attain the optimal beamforming matrix W and solve the non convex problem in Eq. (43). In particular, AO algorithm divides the large problem into a series of sub problems by alternatively minimizing the objective function involving the individual subset of variables. Although AO algorithm has a good error reduction during each iter-

ation, it can be very slow to converge to profoundly accurate solution due to its sensitiveness to the initial value of the variables, high implementation complexity and signaling overhead [42]. We employ the iterative algorithm based on MM approach where it turns a non differentiable problem into a smooth problem. MM algorithm finds a surrogate function that minorizes or majorizes the objective function and then optimizes the surrogate function until the convergence criteria is satisfied. Moreover, MM algorithm guarantees to converge faster than AO algorithm due to low computation complexity (avoids large matrix inversions) and its ability to deal smoothly with inequality and equality constraints. Therefore, we propose an iterative MM (IMM) algorithm based on majorization minimization [36–38] technique to attain \mathbf{W} and also to solve the non-convex design problem in (43), since the objective function $f_{m,n}(\{\mathbf{G}_{m,n}\}_{m=1}^M)$ is concave. Furthermore, we linearize the minorizing term by the following inequality that supports due to the concavity of $\log(x)$ as

$$M(\mathbf{C}, \mathbf{D}) \triangleq \log_2 \det(\mathbf{D}) + \frac{1}{\ln} \text{tr}(\mathbf{D}^{-1}(\mathbf{C} - \mathbf{D})). \quad (47)$$

Finally, we employ the proposed IMM algorithm to provide a sequence of achievable downlink rates for each iteration q . Algorithm 2 summarizes the steps of proposed iterative MM approach to maximize the weighted sum-rate and also solves the non-convex problem given in (43).

Algorithm 2. Proposed IMM Algorithm

1. **Initialize:** $\{\mathbf{G}_{m,n}^{(q)}\}_{m=1}^M \geq 0$, set $q = 1$;
2. **Repeat:**
 - 1: **for** $q \leftarrow q + 1$ **do**
 - 2: update $\{\mathbf{G}_{m,n}^{(q+1)}\}_{m=1}^M$ as a solution to the following convex problem

$$\begin{aligned} \max_{\{\mathbf{G}_{m,n} \geq 0\}_{m=1}^M} & \sum_{m=1}^M B_{m,n} f'_{m,n}(\{\mathbf{G}_{m,n}^{(q+1)}, \mathbf{G}_{m,n}^{(q)}\}_{m=1}^M) \\ \text{s.t.} & \quad \text{tr} \left(\sum_{m=1}^M \mathbf{G}_{m,n}^{(q+1)} \right) \leq P_p. \end{aligned} \quad (48)$$

Until convergence criterion is satisfied.

3: **end for**

3. **Determine:** $W_{m,n} \leftarrow \mathbf{U}_{m,n} \mathbf{T}_{m,n}^{1/2}$ where $\mathbf{m} \in \mathcal{M}$ and $\mathbf{p} \in \mathcal{N}_B$.

In Algorithm 2,

$$\begin{aligned} f'_{m,n}(\{\mathbf{G}_{m,n}^{(q+1)}, \mathbf{G}_{m,n}^{(q)}\}_{m=1}^M) & \triangleq R'_{1,m,n}(\{\mathbf{G}_{m,n}^{(q+1)}, \mathbf{G}_{m,n}^{(q)}\}_{m=1}^M) \\ & + R'_{2,m,n}(\{\mathbf{G}_{m,n}^{(q+1)}, \mathbf{G}_{m,n}^{(q)}\}_{m=1}^M), \end{aligned} \quad (49)$$

where the first and second term in (49) are given in Eqs. (50) and (52) respectively. Eq. (51) is written based on (47) to expand the second term in (50).

$$R'_{1,m,n}(\{\mathbf{G}_{m,n}^{(q+1)}, \mathbf{G}_{m,n}^{(q)}\}_{m=1}^M) \triangleq \log_2 \left(P_{1,m,n} \mathbf{G}_{m,j}^{(q+1)} + \sum_{j=1, j \neq m}^M \mathbf{G}_{m,j}^{(q+1)} + \sigma_{1,m,n}^2 \right) - M \left(\sum_{j=1, j \neq m}^M \mathbf{G}_{m,j}^{(q+1)} + \sigma_{1,m,n}^2, \sum_{j=1, j \neq m}^M \mathbf{G}_{m,j}^{(q)} + \sigma_{1,m,n}^2 \right), \quad (50)$$

$$M \left(\sum_{j=1, j \neq m}^M \mathbf{G}_{m,j}^{(q+1)} + \sigma_{1,m,n}^2, \sum_{j=1, j \neq m}^M \mathbf{G}_{m,j}^{(q)} + \sigma_{1,m,n}^2 \right) \triangleq \log_2 \det \left(\sum_{j=1, j \neq m}^M \mathbf{G}_{m,j}^{(q+1)} + \sigma_{1,m,n}^2 \right) + \frac{1}{\ln} \text{tr} \left(\left(\sum_{j=1, j \neq m}^M \mathbf{G}_{m,j}^{(q+1)} + \sigma_{1,m,n}^2 \right)^{-1} \left(\sum_{j=1, j \neq m}^M \mathbf{G}_{m,j}^{(q)} + \sigma_{1,m,n}^2 - \sum_{j=1, j \neq m}^M \mathbf{G}_{m,j}^{(q+1)} + \sigma_{1,m,n}^2 \right) \right). \quad (51)$$

$$R'_{2,m,n}(\{\mathbf{G}_{m,n}^{(q+1)}, \mathbf{G}_{m,n}^{(q)}\}_{m=1}^M) \triangleq \log_2 \left(P_{2,m,n} \mathbf{G}_{m,j}^{(q+1)} + P_{1,m,n} \mathbf{G}_{m,j}^{(q+1)} + \sum_{j=1, j \neq m}^M \mathbf{G}_{m,j}^{(q+1)} + \Psi + \sigma_{2,m,n}^2 \right) - M \left(P_{1,m,n} \mathbf{G}_{m,j}^{(q+1)} + \sum_{j=1, j \neq m}^M \mathbf{G}_{m,j}^{(q+1)} + \Psi + \sigma_{2,m,n}^2, P_{1,m,n} \mathbf{G}_{m,j}^{(q)} + \sum_{j=1, j \neq m}^M \mathbf{G}_{m,j}^{(q)} + \sum_{c \in \mathcal{N} \setminus \{m\}} \mathbf{E}_{m,c}^{(q)} + \sigma_{2,m,n}^2 \right). \quad (52)$$

In a similar way, we can also derive the second term in Eq. (52). $\mathbf{T}_{m,n}$ represents diagonal matrix which consists of non-zero eigen values and columns in $\mathbf{U}_{m,n}$ denotes the equivalent eigen vectors. We define $\Psi \triangleq \sum_{c \in \mathcal{N} \setminus n} \sum_{m=1}^M \mathbf{E}_{m,c}^{(q+1)}$, $\mathbf{E}_{m,c}^{(q)} \triangleq \hat{\mathbf{g}}_{2,m,c} \mathbf{G}_{m,c}^{(q)} \hat{\mathbf{g}}_{2,m,c}^H$ and $\mathbf{G}_{m,j}^{(q)} \triangleq \hat{\mathbf{h}}_k \mathbf{G}_j^{(q)} \hat{\mathbf{h}}_k^H$ for simplicity. By substituting the value of optimal beamforming vector $W_{m,n}$ obtained from Algorithm 2 in Eq. (12), we can obtain the downlink sum-rate for SVUM. Its good to note that the values attained over the iterations of proposed algorithm are non-decreasing.

6. Numerical results

In this section, the performance of the proposed scheme (proposed JUCPA algorithm and IMM algorithm) is compared with the existing NOMA schemes in [20,22] and the conventional OMA scheme [35] for SVUM. NOMA schemes proposed in [20,22] are evaluated for SVUM referred to as ZFBF scheme and RABF scheme respectively in the sequel. We consider a multicell MIMO-NOMA downlink system as shown in Fig.1. We assume there are 3 cells, $N_B = 3$ base stations, each with two transmit antennas and $N_M = 12$ mobile stations, each equipped with a single receive antenna. Each BS is subject to the same transmit power constraint. Unless otherwise specified, we assume $\gamma = 3$, $\hat{h}_1 = 40$ m, $\hat{h}_2 = 120$ m, $P_{2,m,n} = 0.9$, channel uncertainty (error bound) for SVUM is $\varepsilon = 0.05$, $n_{B,p} = 2$, $\beta = 0$ dB and $\sigma_{m,n}^2 = 1$. We also assume $\hat{h}_1(\hat{h}_2)$ is the distance from the BS to CC (CE) user. We will examine the worst-case average weighted sum-rate (AWSR) performance for SVUM. AWSR was achieved by averaging the sum-rate over the acquisition of fading channel matrices. Unless explicitly stated, all results are presented for 30 channel fading realizations. We consider fixed equal and unequal weights i.e. [1 1]/2 and [2 1]/3 for each cluster. We also presume that the elements of channel matrices between the MS in the b^{th} cell and BS in the a^{th} cell follows independent and identically distributed (i.i.d.) complex gaussian with $\mathcal{CN}(0, \beta^{a-b})$ distribution in which we call β as the inter-cell channel gain. Convergence criteria is set to 10^{-4} , i.e., we consider that the proposed IMM algorithm

comes to halt when the difference between attained AWSR values within the successive iterations are less than 10^{-4} .

In Fig. 4, worst-case AWSR performance is plotted versus BS transmit power (SNR) considering perfect SIC at the receiver. Worst-case AWSR values associated with the proposed scheme for perfect CSI, the proposed scheme for SVUM, ZFBF scheme, RABF scheme and OMA scheme for SVUM are compared. It is observed from results that the sum-rate increases with increase in transmit power for all the schemes. The proposed scheme perform better than the other considered schemes for all transmission power. In particular, at SNR = 20 dB, worst-case AWSR attained by the proposed scheme for SVUM is 18 [bit/c.u.] whereas the ZFBF scheme for SVUM achieves only 17 [bit/c.u.]. This performance gain of 1 [bit/c.u.] is due to the reason that the proposed scheme finds the optimal transmit beamforming vector for each cluster by considering MDF (improves the performance of CE user) and channel correlation as a metric to schedule the users. It is also good to note that the AWSR performance of the proposed scheme for SVUM perform close to the case with perfect CSI.

In Fig. 5, worst-case AWSR performance is plotted versus BS transmit power (SNR) with imperfect SIC at the CC user. Here we consider the small amount of interference $\mu = 0.001$ at the CC user in order to evaluate the impact of the imperfect SIC in the MIMO-NOMA system. It can be observed from the results that the worst-case AWSR is certainly reduced due to the imperfect SIC receiver. At SNR = 20 dB, the proposed scheme for SVUM attains the AWSR performance gain of around 1.2 [bit/c.u] than the ZFBF scheme. It is also good to note that the difference in the AWSR performance gain between the proposed and existing schemes are relatively higher for imperfect SIC compared to ideal (perfect) SIC conditions. This proves the effectiveness of the proposed scheme under the imperfect SIC and the channel uncertainty conditions.

Fig. 6. shows that the worst-case AWSR has been increased by considering unequal priority weights compared to fixed equal weights allocated to CC and CE users present in each cluster. We have evaluated the worst-case AWSR performance by considering equal [1 1]/2 and unequal priority [2 1]/3 weights. In unequal priority weights, larger weights (2/3) are given to CC user and smaller weights (1/3) are given to CE user. This is mainly due to the reason that the achievable rate by the CE user is very less compared to CC

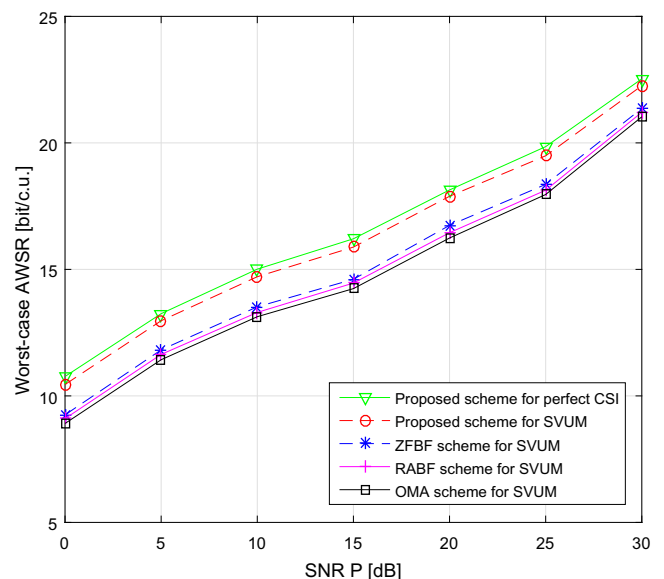


Fig. 5. Worst-case AWSR versus SNR with Imperfect SIC for $\hat{h}_1 = 40$ m, $\hat{h}_2 = 120$ m and $P_{2,m,n} = 0.9$.

user. At SNR = 20 dB, the proposed scheme with unequal weights achieves the performance gain of close to 1 [bit/c.u.] as compared with the proposed scheme for equal weights. This is due to the fact that the CC user is not affected by the ICI and IUI due to its location (closer to the BS) and implementation of SIC respectively.

Fig. 7 illustrates how the distance between the BS and users affects worst-case AWSR for the proposed scheme, ZFBF scheme, JUCPAZF scheme and the conventional OMA scheme. JUCPAZF scheme employs the proposed JUCPA algorithm with the conventional ZF beamforming matrix. We set $\hat{h}_1 = 40$ m and vary \hat{h}_2 . It is noted from the results that when \hat{h}_2 increases, worst-case AWSR decreases for all the considered schemes. We also note that proposed NOMA scheme outperform the ZFBF scheme, JUCPAZF scheme and the conventional OMA scheme. In particular, the proposed scheme for SVUM achieves AWSR performance gain of close to 1.1 [bit/c.u.] in the entire distance region compared to the ZFBF scheme. Interestingly, JUCPAZF scheme performs better than the ZFBF scheme for the entire distance clearly showing the effectiveness of our proposed JUCPA algorithm. When $\hat{h}_2 = 100$ m, the AWSR performance gap between the proposed NOMA scheme and the conventional OMA scheme is 0.8 [bit/c.u.], while the performance gap increases close to 2 [bit/c.u.] at $\hat{h}_2 = 200$ m. This can be justified by the fact that the frequency and energy resources designated to the CE user are lost in the conventional OMA, whereas more transmission power allocated to such users in the proposed NOMA scheme increases their achievable rate.

We examine the impact of power allocation coefficient of CE user on depicting the fairness between CC and CE user in Fig. 8. It can be observed that the fairness between CC and CE users increases while increasing the power allocation coefficient of CE users for all three considered schemes. This is due to the fact that CE users which are located near the boundary of the cellular network generally tend to have the weaker channel conditions. So, BS allocates higher power for CE users to improve their achievable rate which in turn enhance the user fairness. Additionally, the proposed scheme for SVUM consistently outperforms the ZFBF and RABF scheme for the unified range. In particular, the user fairness index for the proposed scheme has been increased by 0.08 compared to the ZFBF scheme since the proposed scheme mitigates the ICI (caused by allocating more power) experienced by CE users.

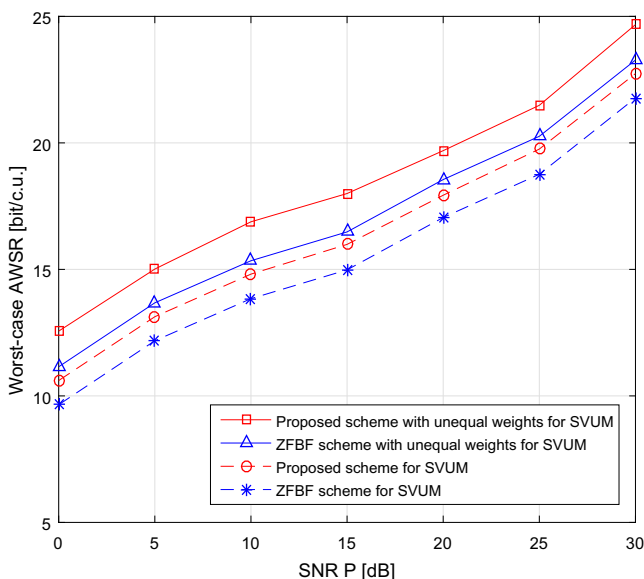


Fig. 6. Worst-case AWSR versus SNR with Unequal weights for $\hat{h}_1 = 40$ m, $\hat{h}_2 = 120$ m and $P_{2,m,n} = 0.9$.

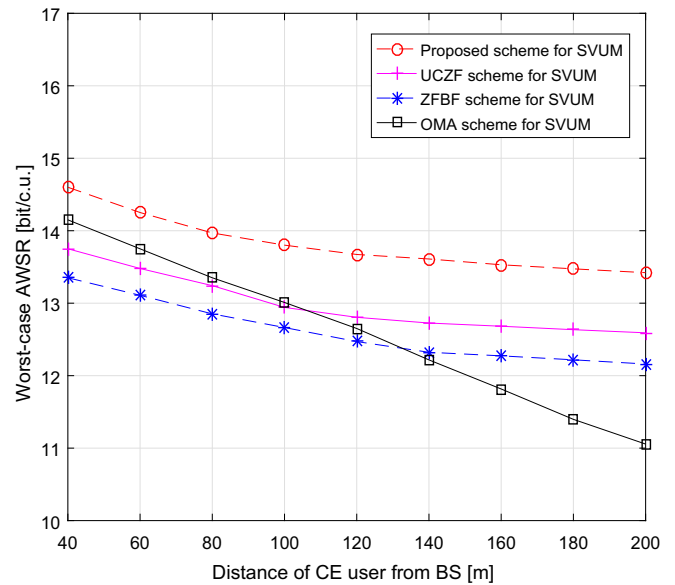


Fig. 7. Worst-case AWSR versus distance of CE user (\hat{h}_2) for SNR = 5 dB and $\hat{h}_1 = 40$ m

It's also good to note that the user fairness of the RABF scheme outperforms the ZFBF scheme.

Fig. 9 exemplifies the effect of uncertainty values on the worst-case AWSR with $\beta = 0$ dB. Simulations are carried out for 20 iterations at SNR = 10 dB. It can be noticed that the worst-case AWSR value decreases for all the considered schemes while increasing the channel uncertainty. Results from Fig. 6 emphasize that the proposed scheme performs better than the ZFBF scheme and the conventional OMA scheme for the entire range of uncertainty $\epsilon_{m,n}$ values. At $\epsilon_{m,n} = 0.05$, the proposed scheme achieves AWSR performance gain of 1 [bit/c.u.] as compared with the ZFBF scheme. This was expected because the proposed IMM algorithm is designed in such a way to obtain the optimal beamforming matrix even in the worst-case conditions.

We plot worst-case AWSR versus the inter-cell channel gain β with SNR = 10 dB in Fig. 10. Results obtained illustrate that our proposed scheme performs exceedingly well for the unified range

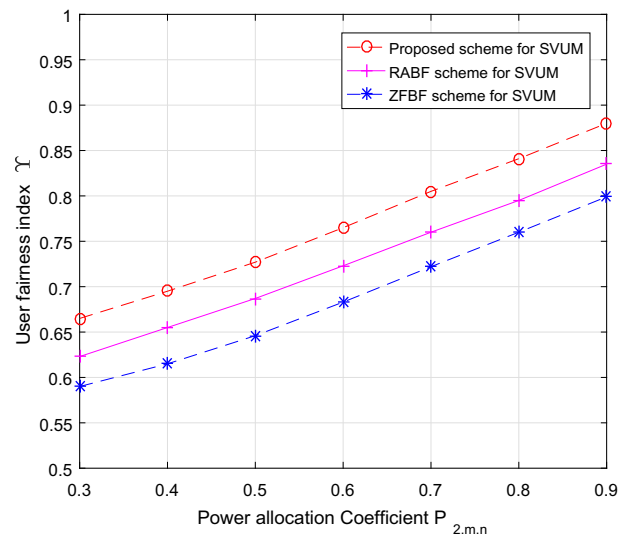


Fig. 8. Worst-case AWSR versus power allocation coefficient for SNR = 10 dB, $\hat{h}_1 = 40$ m and $\hat{h}_2 = 120$ m.

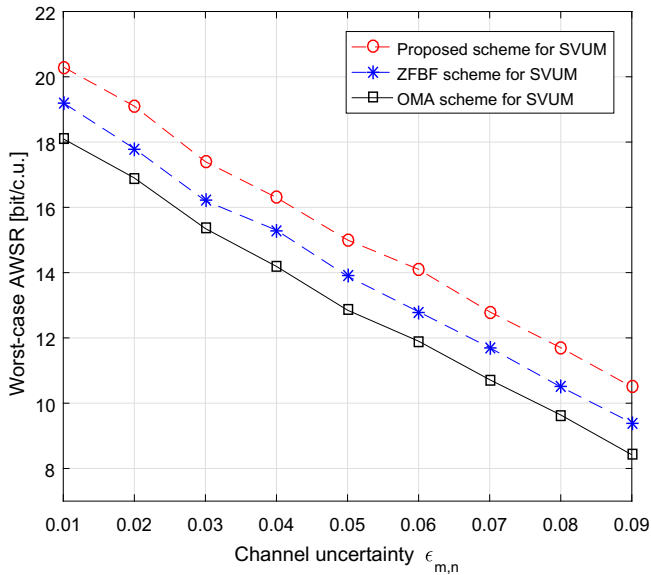


Fig. 9. Worst-case AWSR versus uncertainty ϵ for iterations = 30, SNR = 10 dB and $P_{2,m,n} = 0.9$.

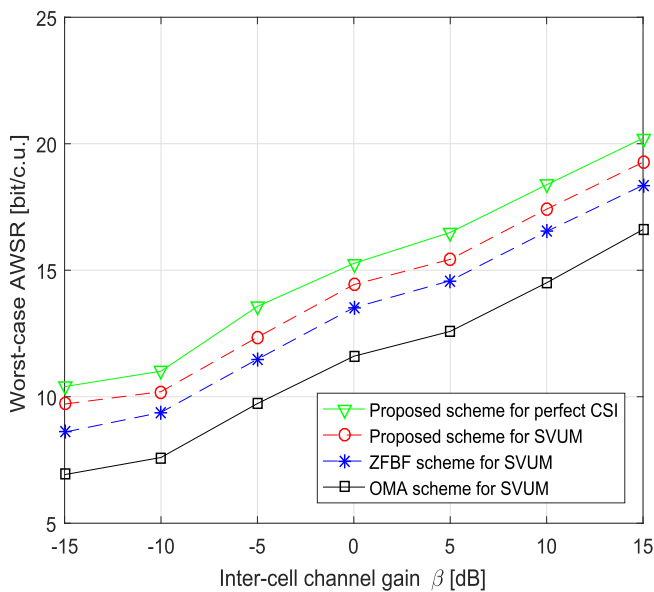


Fig. 10. Worst-case AWSR versus inter-cell channel gain for SNR = 10 dB, $h_1 = 40$ m and $h_2 = 120$ m.

of β as compared with the ZFBF scheme and the conventional OMA scheme. When $\beta = -5$ dB, the proposed scheme achieves AWSR performance gain of 0.9 [bit/c.u.] as compared with the ZFBF scheme. This observance can be elucidated by taking into account that the ZFBF scheme performs well only when single BS is present and it is also worth to mention that as β decreases, multicell system advances to a system composed of N_B parallel single cell networks. Moreover, the proposed scheme consistently outperforms the conventional OMA scheme for all the values of β .

7. Conclusion

In this paper, a robust beamforming design was examined to solve the WSRM problem in multicell MIMO-NOMA system with the imperfect CSI at BSs for 5G communications. In particular, we

have considered the SVUM for the inclusion of CSI errors. We have proposed an efficient JUCPA algorithm which considers MDF and channel correlation to select the best user pair as a cluster. The proposed JUCPA algorithm not only maximize the worst-case WSR but also reduces IUI and ICRI. We have also proposed an IMM algorithm based on MM technique to find the optimal transmit beamforming matrix that further enhance the worst-case WSR and also solve the objective problem formulated with SVUM. Via numerical results, it was confirmed that the AWSR achieved by the proposed scheme for NOMA consistently outperforms the AWSR attained by the existing NOMA schemes and the conventional OMA scheme. Furthermore, the proposed scheme reduces ICI and also ensure the best user fairness compared to the ZFBF and RABF scheme.

Acknowledgment

This work was supported by Brain Korea 21 Plus (BK 21+), Ministry of Education, Science and Technology (MEST) 2015R1A2A1A05000977, National Research Foundation (NRF), South Korea.

References

- [1] Andrews JG, Buzzi S, Choi W, Hanly SV, Lozano A, Song ACK, Zhang JC. What will 5G be? *IEEE J Sel Areas Commun* 2014;32(6):1065–82.
- [2] Chih-Lin I, Corbett R, Shuangfeng H, Zhikun X, Gang L, Pan Zhengang. Towards green and soft: a 5G perspective. *IEEE Commun Mag* 2014;52(2):66–73.
- [3] Al-Samman AM, Rahman TA, Azmi MH, Hindia MN. Large-scale path loss models and time dispersion in an outdoor line-of-sight environment for 5G wireless communications. *AEU - Int J Electron Commun* 2016;70(11):1515–21.
- [4] Ashraf N, Haraz OM, Ali MMM, Ashraf MA, Alshebili SAS. Optimized broadband and dual-band printed slot antennas for future millimeter wave mobile communication. *AEU - Int J Electron Commun* 2016;70(3):257–64.
- [5] Benjebbour A, Li A, Saito Y, Kishiyama Y, Harada A, Nakamura T. System-level performance of downlink NOMA for future LTE enhancements. In *Proc. IEEE Global Commun. Conf.*; 2013. p. 66–70.
- [6] Abuibaid MA, Çolak SA. Energy-efficient massive MIMO system: exploiting user location distribution variation. *AEU - Int J Electron Commun* 2017;72:17–25.
- [7] Marinello JC, Abrão T. Pilot distribution optimization in multi-cellular large scale MIMO systems. *AEU - Int J Electron Commun* 2016;70(8):1094–103.
- [8] Islam SR, Avazov N, Dobre OA, Kwak KS. Power-domain non-orthogonal multiple access (NOMA) in 5G systems: potentials and challenges. *IEEE Commun Surv Tutor* 2016.
- [9] Dai L, Wang B, Yuan Y, Han S, Chin-Lin I, Wang Z. Non-orthogonal multiple access for 5G: solutions, challenges, opportunities, and future research trends. *IEEE Commun Mag* 2015;53(9):74–81.
- [10] Wunder G, Jung P, Kasparick M, Wild T, Schaich F, Chen Y, Ten Brink S, Gaspar I, Michailow N, Festag A, Mendes L. 5G NOW: non-orthogonal, asynchronous waveforms for future mobile applications. *IEEE Commun Mag* 2014;52(2):97–105.
- [11] Saito Y, Kishiyama Y, Benjebbour A, Nakamura T, Li A, Higuchi K. Non-orthogonal multiple access (NOMA) for cellular future radio access. In *Proc. IEEE Veh. Techn. Conf.*; 2013. p. 1–5.
- [12] Higuchi K, Kishiyama Y. Non-Orthogonal access with random Beamforming and intra-beam SIC for cellular MIMO downlink. In *Proc. IEEE Veh. Techn. Conf.*; 2013. p. 1–5.
- [13] Ding Z, Peng M, Poor HV. Cooperative non-orthogonal multiple access in 5G systems. *IEEE Commun Lett* 2015;19(8):1462–5.
- [14] Choi J. Non-orthogonal multiple access in downlink coordinated twopoint systems. *IEEE Commun Lett* 2014;18(2):313–6.
- [15] Benjebbour A, Saito K, Li A, Kishiyama Y, Nakamura T. Nonorthogonal multiple access (NOMA): concept, performance evaluation and experimental trials. In *Proc. IEEE Intern. Conf. Wireless Networks and Mobile Commun.*; 2015.
- [16] Choi J. Minimum power multicast beamforming with superposition coding for multiresolution broadcast and application to NOMA systems. *IEEE Trans Commun* 2015;63(3):791–800.
- [17] Ding Z, Adachi F, Poor HV. The application of MIMO to non-orthogonal multiple access. *IEEE Trans Wireless Commun* 2016;15(1):537–52.
- [18] Sun Q, Han S, Xu Z, Wang S, Chih-Lin I, Pan Z. Sum rate optimization for MIMO non-orthogonal multiple access systems. In *Proc. IEEE Wireless Commun. and Networking Conf.*; 2015. p. 747–52.
- [19] Lei L, Yuan D, Ho CK, Sun S. Joint optimization of power and channel allocation with non-orthogonal multiple access for 5G cellular systems. In *Proc. IEEE Global Commun. Conf.*; 2015. p. 1–6.

- [20] Kim B, Lim S, Kim H, Suh S, Kwun J, Choi S, Lee C, Lee S, Hong D. Non-orthogonal multiple access in a downlink multiuser beamforming system. In: Proc. IEEE Mil. Commun. Conf.; 2013. p. 1278–83.
- [21] Al-Abbasi ZQ, So DKC. Power allocation for sum rate maximization in non-orthogonal multiple access system. In Proc. IEEE PIMRC; 2015. p. 1839–43
- [22] Higuchi K, Kishiyama Y. Non-orthogonal multiple access using intra-beam superposition coding and successive interference cancellation for cellular MIMO downlink. IEICE Trans Commun 2015;98(9):1888–95.
- [23] Hanif MF, Ding Z, Ratnarajah T, Karagiannidis GK. A minorization-maximization method for optimizing sum rate in the downlink of non-orthogonal multiple access systems. IEEE Trans Signal Process 2016;64(1):76–88.
- [24] Zhang X, Palomar DP, Ottersten B. Statistically robust design of linear MIMO transceivers. IEEE Trans Signal Process 2008;56(8):3678–89.
- [25] Shenouda M, Davidson T. On the design of linear transceivers for multiuser systems with channel uncertainty. IEEE J Sel Areas Commun 2008;26(6):1015–24.
- [26] Loyka S, Charalambous CD. On the compound capacity of a class of MIMO channels subject to normed uncertainty. IEEE Trans Information Theory 2012;58(4):2048–63.
- [27] Yang K, Huang J, Wu Y, Wang X, Chiang M. Distributed robust optimization (DRO) Part I: framework and example. J Optim Eng 2014;15(1):35–67.
- [28] Pascual-Iserte A, Palomar DP, Perez-Neira AI, Lagunas MA. A robust maximin approach for MIMO communications with imperfect channel state information based on convex optimization. IEEE Trans Signal Process 2006;54(1):346–60.
- [29] Yang Z, Ding Z, Fan P, Karagiannidis GK. On the performance of non-orthogonal multiple access systems with partial channel information. IEEE Trans Commun 2016;64(2):654–67.
- [30] Ding Z, Yang Z, Fan P, Poor H. On the performance of nonorthogonal multiple access in 5G systems with randomly deployed users. IEEE Signal Process Lett 2014;21(12):1501–5.
- [31] Sun Q, Han S, Chin-Lin I, Pan Z. On the ergodic capacity of MIMO NOMA systems. IEEE Wireless Commun Lett 2015;4(4):405–8.
- [32] Timotheou S, Krikidis I. Fairness for non-orthogonal multiple access in 5G systems. IEEE Signal Process Lett 2015;22(10):1647–51.
- [33] Ding Z, Poor HV. Design of massive-MIMO-NOMA with limited feedback. IEEE Signal Process Lett 2016;23(5):629–33.
- [34] Ding Z, Fan P, Poor HV. Impact of user pairing on 5G nonorthogonal multiple access downlink transmissions. IEEE Trans Veh Technol 2016;65(8):6010–23.
- [35] Tse D, Viswanath P. Fundamentals of wireless communication. Cambridge University Press; 2005.
- [36] Hunter DR, Lange K. A tutorial on MM algorithms. Am Stat 2004;58:30–7.
- [37] Stoica P, Selen Y. Cyclic minimizers, majorization techniques, and the expectation-maximization algorithm: a refresher. IEEE Signal Process Mag 2004;21(1):112–4.
- [38] Hunter DR. MM algorithms for generalized Bradley-Terry models. Ann Stat 2004;32(1):384–406.
- [39] Jain R, Chiu D, Hawe W. A quantitative measure of fairness and discrimination for resource allocation in shared computer systems, DEC Technical Report 301, vol. 38; 1984.
- [40] Otao N, Kishiyama Y, Higuchi K. Performance of non-orthogonal access with SIC in cellular downlink using proportional fair-based resource allocation. In: Proc. IEEE Wireless Commun. Systems.; 2012. p. 476–80.
- [41] Saito Y, Kishiyama Y, Benjebbour A, Nakamura T, Li A, Higuchi K. Non-orthogonal multiple access (NOMA) for cellular future radio access. In: Proc. IEEE Veh. Techn. Conf.; 2013. p. 1–5.
- [42] Bezdek JC, Hathaway RJ. Convergence of alternating optimization. Parallel Sci Comput 2003;11(4):351–68.
- [43] C.D. Charalambous, S.Z. Denic, S.M. Djouadi, Robust capacity of white Gaussian noise channels with uncertainty. in Proc. IEEE in Decision and Contrl. Conf., vol. 5; Dec. 2004. pp. 4880–84.
- [44] Vandenberghe L, Boyd S. Semidefinite programming. SIAM Rev 1996;38(1):49–95.